Green Chemistry

Accepted Manuscript

ROYAL SOCIETY OF CHEMISTRY

www.rsc.org/greenchem

Journal Name

RSCPublishing

ARTICLE

Expanding the scope of enzymatic carboligation reactions in flow-mode: production of optically active tertiary alcohols with packed-bed micro-bioreactors

P. P. Giovannini,*[a] O. Bortolini,[a] A. Cavazzini,[a] R. Greco,[a] G. Fantin and A. Massi*[a]

Cite this: DOI: 10.1039/x0xx00000x

Received 00th January 2012,
Accepted 00th January 2012

DOI: 10.1039/x0xx00000x

www.rsc.org/

Acetylacetoin synthase (AAS) from *Bacillus licheniformis* has been partially purified and immobilized on silica support and its activity tested under batch conditions in the homo-coupling of a set of α-diketones leading to valuable α-hydroxy ketone derivatives displaying a chiral tertiary alcohol functionality at the α-position. Next, the effectiveness of AAS heterogeneous catalysis has been evaluated under continuous-flow conditions by fabricating the corresponding packed-bed microreactors (pressure-resistant stainless-steel columns). It has been demonstrated that the covalent immobilization on silica support and the flow regime synergistically contribute to preserve the enzyme activity over time, thus permitting the long-term operation (up to 15 days) of the prepared bioreactors for the production of the chiral targets *via* the umpolung strategy.

Introduction

In current years continuous-flow asymmetric catalysis has been emerging as an attractive field of research in academic and industrial laboratories.[1] Following a critical and comprehensive cost analysis, the production of chiral organic synthons and fine chemicals by operation of meso- and micro-flow devices may offer several advantages over conventional batch reactors, including safety and sustainability of the processes, direct scalability, and ease of automation and integration with in-line analysis methods.[2] Heterogeneization of homogenous chiral catalysts represents an effective strategy towards process implementation because of simple product/catalyst separation and catalyst recycling opportunities.[1a,c,3] Recently, our[4] and other groups[5] have demonstrated that heterogeneous organocatalysis in combination with flow technologies constitutes an efficient synthetic platform for the production of chiral target molecules, being the absence of metal contamination an additional and peculiar benefit of the synthetic strategy.

The design of asymmetric organocatalytic processes is often inspired by the mechanisms of enzyme catalysis with the aim to reproduce nature achievements in terms of chemo- and stereo-selectivity of the investigated synthesis.[6] Outstanding results in this direction have been obtained even in flow conditions;[1] nevertheless, it is a matter of fact that, to date, biocatalytic approaches still remain the preferred choice of chemical and pharma industries for the continuous-flow production of chiral molecules.[7] Biocatalytic processes, in fact, are unique in several ways: they occur under very mild conditions (pH and temperature), with high atom and stereochemical efficiency, and with diminished environmental concerns.[8] Immobilization of biocatalysts (enzymes and whole cells) together with their use in flow-regime is frequently the key for success of industrial and lab-scale syntheses.[9] Typical advantages of this approach are improved biocatalyst stability and increased activity for those enzymes subjected to product inhibition thanks to the continuous elution of reaction mixtures. Immobilization strategies comprise covalent bonding to organic or inorganic solid supports, encapsulation, entrapment, and adsorption (specific and non-specific) methods.[10] In most cases, the fixed-bed configuration, in the form of either packed or monolithic column, is the optimal choice for biocatalytic flow processes, overcoming the continuous stirred reactor set-up in terms of volumetric productivities.[7b,11] Therefore, microstructured fixed-bed bioreactors can be envisaged as useful scale-down systems for the fast screening of realistic flow process conditions.

Dominant in the field of (micro)flow biocatalysis is the utilization of hydrolases and oxidoreductases in single- and multiple-reactor processes,[1a,d,e,12,13] while more limited is the number of strategies involving the challenging asymmetric formation of carbon-carbon bonds (Figure 1).[14-16] Optically active cyanohydrins (Figure 1, **I**) have been prepared from aldehydes using hydroxynitrile lyases (HNL) in both chip and column reactors (eq. *a*).[14] Recently, immobilized aldolases (e.g. fructose-1,6-diphosphate aldolase, RAMA) have been reported to promote the addition of dihydroxyacetone phosphate to aldehydes yielding phosphorylated α,β-dihydroxy ketones (Figure 1, **II**) as intermediates of the flow synthesis of complex chiral carbohydrates (eq. *b*).[15] Also, several thiamine diphosphate (ThDP)-dependent enzymes such as benzaldehyde lyase (BAL), benzoylformate decarboxylase (BFD), pyruvate decarboxylase (PDC), and transketolase (TK) have been

successfully utilized in different flow chemistry programs for the production of target molecules incorporating the chiral α-hydroxy ketone functionality (Figure 1, **III**) as common structural motif (eq. *c*).[16] It appears evident from the above survey that expanding the enzyme toolbox to access valuable chiral frameworks by biocatalytic continuous-flow carboligations is of timely significance. In this article we report on the flow synthesis of chiral tertiary α-hydroxy ketones (Figure 1, **IV**) from α-diketones by operating fixed-bed microreactors fabricated with acetylacetoin synthase (AAS)-functionalized packing material (eq. *d*). The α-hydroxy ketone group **IV** displaying a chiral tertiary alcohol functionality at the α-position is the key feature of range of natural products and antibiotics,[17] but also a densely functionalized building block for the asymmetric synthesis of important organic molecules such as diols, amino alcohols, and so forth.[18] Despite its synthetic utility and significance, the chiral quaternary structure **IV** is hardly accessible through direct, purely chemical approaches;[19] instead, straightforward routes to derivatives of type **IV** are realized with the ThDP-dependent enzymes AAS[20] and YerE,[21] which efficiently catalyze the formal carboligation of an aldehyde with a ketone through diketone-diketone and pyruvate-ketone couplings, respectively.

In a recent study we have described the continuous-flow, biomimetic synthesis of tertiary alcohols **IV** in racemic form using thiazolium-functionalized polystyrene monolithic microreactors.[4a] Herein, we demonstrate that the same derivatives **IV** can be produced with high enantioselectivities (up to 91% ee) and comparable level of productivity with AAS covalently-bound to mesoporous silica as the catalytic material of fixed-bed microreactors. Significantly, an elevated operational stability was observed for these bioreactors, which were continuously operated for more than 15 days without any significant decrease of enzyme activity.

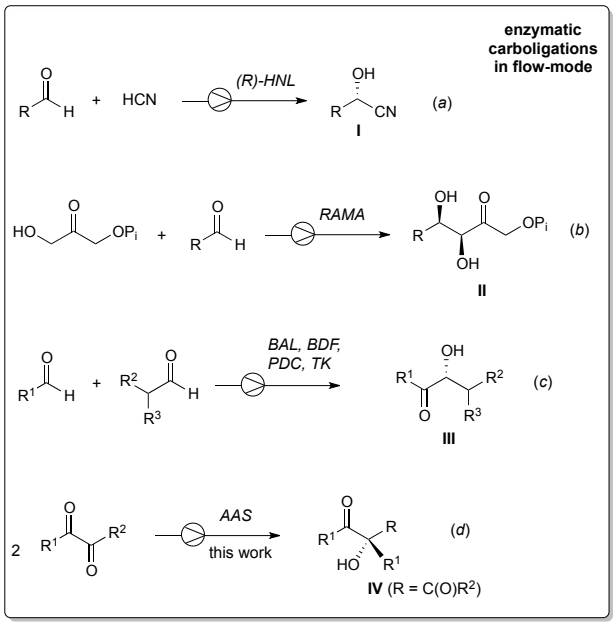

Figure 1 Enzyme tool box for continuous-flow biocatalytic carboligation reactions.

Results and discussion

Acetylacetoin synthase (AAS) from *Bacillus licheniformis* is a 'new'[21b] ThDP-dependent enzyme capable to promote the umpolung (polarity reversal) of α-diketones **1** with high substrate specificity. Distinctive of AAS catalysis is the release of a carboxylic acid molecule in the key hydrolytic step leading to the reactive acyl anion equivalent, whose attack on a second molecule of α-diketone **1** yields the chiral α-hydroxy-β-diketone **2** together with minor amounts of the regioisomeric prochiral derivative **3** (Scheme 1).[20a]

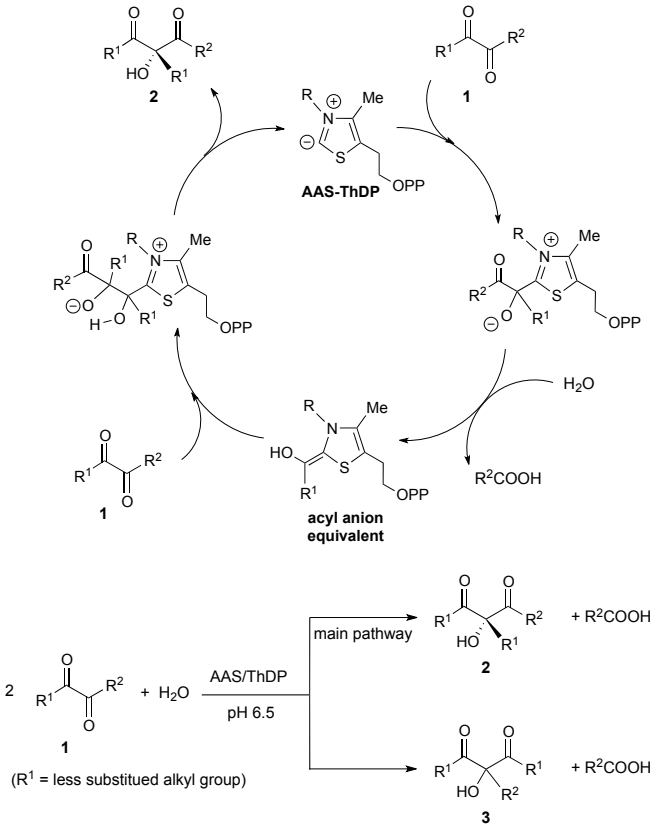

Scheme 1 AAS-catalyzed formation of chiral tertiary alcohols.

AAS-catalyzed homo- and cross-coupling reactions of α-diketones **1** have been previously investigated by our group under conventional batch conditions using *Bacillus licheniformis* crude cell extracts.[20] Although this procedure was quite efficient for the preparation of tertiary alcohols **2** (yields: 30-68%; enantioselectivities: 44-91%), the purification of AAS was first addressed in this study with the hope to achieve a high volumetric activity (U g^{-1}) for the heterogenized enzyme and improved stereoselectivities. Thus, AAS from acetoin-grown cells was partially purified 17-fold by a two-step procedure with 67% recovery of enzyme activity as determined using the homo-coupling of 2,3-pentanedione **1a** as the activity test (Tables 1 and 3). Initially, proteins precipitated between 40-60% ammonium sulfate saturation were tested showing a 4.2-fold enzyme enrichment and total activity recovery. Next, the precipitated proteins were dissolved in phosphate buffer (50 mM, pH 7.0) and chromatographed on a DEAE-Sepharose column with a step gradient of NaCl.

Table 1. Purification of acetylacetoin synthase (AAS) from of *B. licheniformis* DSM13.

Step	Volume (mL)	Total Protein (mg)[a]	Total Activity (U)[b]	Specific Activity (U mg^{-1})	Purification (-fold)[c]	Recovery (%)[d]
Crude extract	26	314	1.8	5.7×10^{-3}	-	100
Ammonium sulfate precipitation	6	75	1.8	2.4×10^{-2}	4.2	100
DEAE chromatography	10	12	1.2	0.10	17.5	67

[a]Protein amount was determined by spectrophotometric UV measurements at 215 and 280 nm (see the Experimental Section and Ref. 30). [b]One unit (U) is defined as the enzyme amount catalyzing the formation of 1 μmol of products **2a** + **3a** in one minute from 2,3-pentanedione **1a**. [c]Ratio between the specific activity of the partially purified enzyme and crude extract. [d]Referred to the total activity recovery.

The active fractions were collected and treated with ammonium sulfate (80% saturation); native polyacrylamide gel electrophoresis indicated AAS as the main component of the precipitated fraction (Figure 2), whose specific activity (0.1 units per mg) remained unchanged for at least one month under storage at 4 °C.

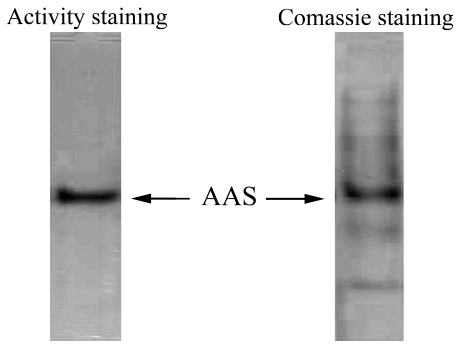

Figure 2 Native gel electrophoresis of partially purified acetylacetoin synthase. Samples were applied to 4% (w/v) polyacrylamide gel and stained with diacetyl-DCPIP-thiazolyl blue mixture (activity staining) and with Comassie brilliant blue (Comassie staining).

Having in mind the utilization of heterogeneous AAS under flow conditions as the ultimate goal of this study, an enzyme covalent immobilization method was next investigated. Indeed, out of different approaches, the covalent attachment of an enzyme to a functionalized solid support is undoubtedly one of the most efficient strategies to enhance protein stability and prevent protein leaching during elution;[10,22] on the other hand, these are critical issues that must be carefully considered to ensure flow bioreactors with long operational stability. Hence, mesoporous silica was chosen as the support and the classical glutaraldehyde method as the immobilization technique.[23] This involved three sequential steps: amino-silanization of silica, derivatization of surface amino groups with glutaraldehyde, and immobilization of partially purified AAS via the free aldehyde groups. Accordingly, 3-aminopropyl-silica was freshly prepared with a satisfactory loading (0.32 mmol g^{-1}) by treatment of mesoporous silica (particle size: 5 μm; pore size 30 nm) with 3-aminopropyl triethoxysilane in refluxing toluene (Scheme 2). Screening of optimal pH conditions for the coupling steps was carried out with reaction buffers in the pH range 5.0 to 8.0. Thus, aminopropyl-silica was suspended in phosphate buffer (pH 7.0), treated with excess glutaraldehyde for 2 h at 30 °C, and then washed. To the activated carrier was then added a solution of AAS in the proper buffer (enzyme/carrier ratio (w/w) = 0.12:1) and the coupling was continued for additional 2 h at 30 °C. Protein mass balance was determined by evaluating the protein concentration left in the solution after the anchoring step. As shown in Figure 3, while an increase of pH corresponded to a decrease of immobilized AAS, the highest volumetric activity (2.9 U/g carrier) was detected at pH 6; under these conditions 78 mg of AAS were bound to one gram of silica support.

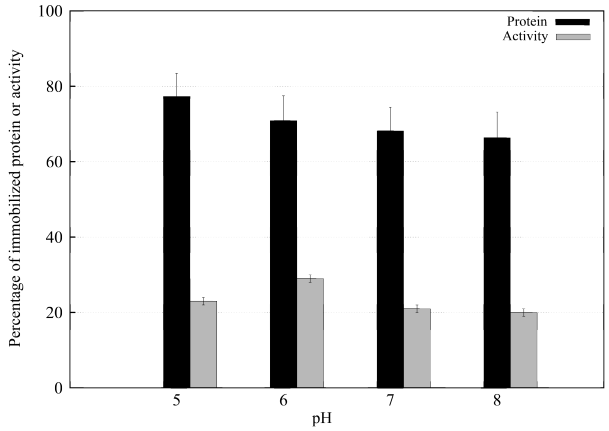

Figure 3. Effect of the immobilization pH on the percentage amount (black histogram) and percentage activity (grey histogram) of immobilized AAS relative to the starting carrier-free enzyme.

Selection of the suitable enzyme/carrier (E/C) ratio (w/w) was next performed by dedicated coupling experiments performed as described before at the optimal pH 6 (Table 2).

Table 2. Effect of the enzyme/carrier ratio (E/C) on the activity of immobilized AAS.

Entry	Initial Activity (U)[a]	Initial Protein (mg)[b]	E/C ratio (mg/g)[c]	Volum. Activity (U/g)[a,d]	Imm. Protein (mg/g)[e]
1	2.5	25	0.025	1.0	25
2	5	50	0.05	1.5	50
3	10	100	0.1	1.9	91
4	20	200	0.2	3.5	160
5	40	400	0.4	2.3	221

[a]Activity (U) of the free enzyme in the starting solution before immobilization. One unit (U) is defined as the enzyme amount catalyzing the formation of 1 μmol of products **2a** + **3a** in one minute from 2,3-pentanedione **1a**. [b]Protein amount in the starting solution as determined by spectrophotometric UV measurements at 215 and 280 nm (see the Experimental Section and Ref. 30). [c]Values normalized to 1 g of aminopropyl-silica. [d]Volumetric activity. [e] Immobilized protein. Protein mass balance was determined by evaluating the protein concentration left in the solution after the anchoring step.

Treatment of activated aminopropyl-silica with increasing amounts of AAS resulted in catalytic materials with progressively higher volumetric activities (up to 3.5 U g^{-1}, entries 1-4). This trend, however, reversed with enzyme/carrier ratios exceeding the critical 0.2 value (entry 4). According to similar immobilization studies,[24] this loss of efficiency may be attributed to the increase of steric hindrance on support preventing access of the substrate to the immobilized enzyme.[25]Alternatively, high protein concentration might be responsible for the formation of multi-covalent linkages between the enzyme and the carrier, thus affecting the structure and activity of the native enzyme.[26]

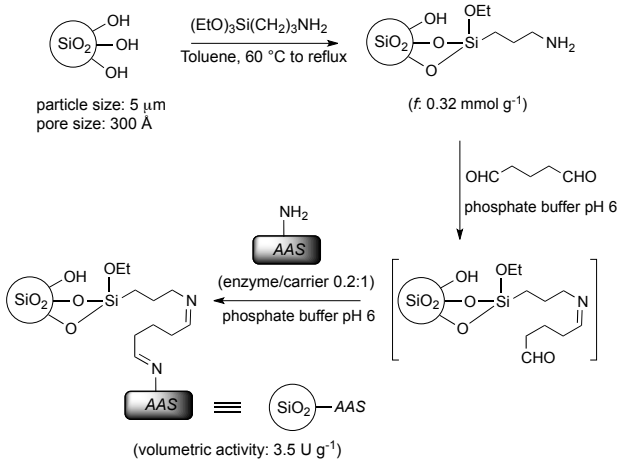

Scheme 2 Optimized procedure for the immobilization of AAS on silica support.

Quite surprisingly, sodium cyanoborohydride reducing treatment of immobilized AAS produced a marked decrease in volumetric activity (*ca.* 80%), which was not compensated for by an increase of enzyme stability (see the Experimental Section). Finally, the effect of pH on the activity of free and immobilized AAS was determined in the pH range 5.0–8.0, and the results are shown in Figure 4. The maximum value of relative activity was observed at pH 6.5 for the free and immobilized enzyme; overall, the absence of a significant pH shift in the two curves seems to be in accordance with no interaction between AAS and the silica support.[27]

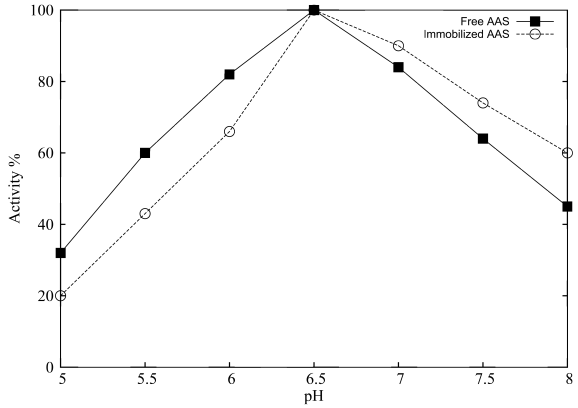

Figure 4. Effect of pH on the activity of free (black line) and immobilized AAS (grey line).

The synthetic value of AAS heterogeneous catalysis was first evaluated in standard batch reactors (Table 3). Accordingly, different portions of AAS-functionalized silica (250 mg) were obtained with the optimal volumetric activity (3.5 U g^{-1}) and utilized in the homo-coupling (1 mmol scale) of unsymmetrically substituted diketones **1a-e** (entries 1-5) and symmetric diketones **1f,g** (entries 6 and 7). In all the investigated cases, immobilized AAS showed the same level of activity of the free enzyme affording the target tertiary alcohols **2a-e** with comparable conversion efficiencies (35-58%, 16 h reaction time) and enantioselectivities (55-91% ee, *R*).[20a] Appreciably, the enantiomeric purity of **2a-e** was, on average, significantly higher (*ca.* 15%) than that detected with the not purified free enzyme.[20]

Table 3. AAS heterogeneous catalysis under batch conditions.[a]

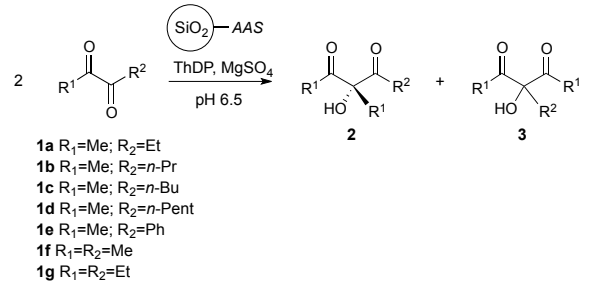

Entry	Diketone **1**	Chiral Alcohol **2** (*ee* [%])[b]	Alcohol **3**	**2** + **3** (*Yield* [%])[c]
1	**1a**	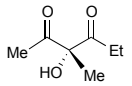 **2a** (85)	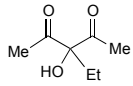 **3a**	46+35
2	**1b**	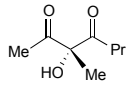 **2b** (91)	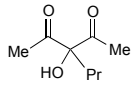 **3b**	48+22
3	**1c**	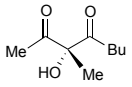 **2c** (72)	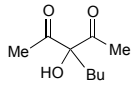 **3c**	45+19
4	**1d**	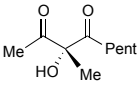 **2d** (55)	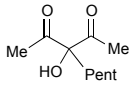 **3d**	58+13
5	**1e**	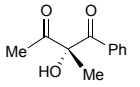 **2e** (80)	-	35+0
6	**1f**	-	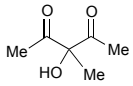 **3f**	0+85
7	**1g**	-	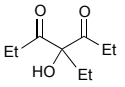 **3g**	0+78

[a]See the Experimental Section. [b]Determined by chiral GC analysis. [c]Isolated yield.

It is also important to point out that while the AAS-promoted coupling of diketones **1f,g** affords symmetrically substituted tertiary alcohols **3f,g**, these prochiral derivatives can be efficiently elaborated into valuable chiral molecules such as α-alkyl-α,β-dihydroxy ketones with high levels of stereocontrol.[18]

Table 4. AAS heterogeneous catalysis under flow conditions.[a]

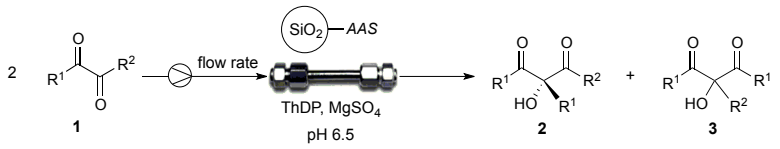

Entry	**1** (*c* [mM])	Flow rate [μL min^{-1}]	Residence Time[b] [min]	Temperature [°C]	**2** + **3**[c] (*Conv.* [%])	**2**[d] (*ee* [%])	*Productivity*[e] [mmol d^{-1}]
1	**1a** (10)	5	56	30	56 + 43	85	0.07
2	**1a** (10)	10	28	30	44 + 34	85	0.11
3	**1a** (10)	15	19	30	33 + 25	85	0.13
4	**1a** (10)	30	9	30	28 + 21	85	0.21
5	**1b** (10)	10	28	30	47 + 23	91	0.10
6	**1c** (10)	10	28	30	46 + 20	74	0.10
7	**1d** (10)	10	28	30	48 + 15	55	0.09
8	**1e** (5)	10	56	30	51 + 0	81	0.02
9	**1f** (10)	10	28	30	0 + 88	-	0.13
10	**1g** (10)	10	28	30	0 + 81	-	0.12

[a]See the Experimental Section for a description of the experimental setup. [b]Calculated residence time. [c]Instant conversions in steady-state regime as established by GC analysis. [d]Determined by chiral GC analysis. [e]Productivities are measured in mmol (**2**+**3**) d^{-1}.

A final and crucial result of this batch investigation was that heterogeneous AAS could be re-used after reactivation with ThDP ten times for repeat or different couplings without any loss of activity.

The success in the above recycle experiment paved the way to the use of ASS-functionalized silica as the packing material of fixed-bed bioreactors with potential long-term stability. Enzyme immobilization was performed under flow conditions ('in situ' immobilization technique) with the fully assembled microreactor.[28] This consisted of a stainless steel column (100 mm length, 2.1 mm internal diameter) slurry packed (toluene) with the previously prepared 3-aminopropyl silica.

Main features of the column were determined by pycnometry and included the hold-up (dead) volume (V_0 = 250 μL), and the total porosity (0.72). The packing amount of spherical silica (240 mg) was calculated by weighing the column before and after filling. After characterization, the column was conditioned with phosphate buffer (pH 7.0), flushed with glutaraldehyde solution, equilibrated to pH 6.0, and finally eluted with AAS solution to obtained the AAS-functionalized catalytic bed (see the Experimental Section). Continuous-flow experiments were performed by first considering the homo-coupling of 2,3-pentanedione **1a** (Table 4, entries 1-4). It turned out from preliminary tests that the preparation of a fully homogeneous 10 mM solution of **1a** containing 0.04 mol% of ThDP and $MgSO_4$ (0.08 mol%) required the addition of DMSO (1% w/v), and that utilization of triethanolamine buffer (pH 6.5) gave feed solutions of **1a** with longer stability (25 °C, air) compared to the corresponding solutions prepared in phosphate buffer.[29] The optimal reaction mixture was then pumped at different flow rates through the bioreactor to evaluate the influence of the residence time on conversion efficiency (%) and productivity (mmol d^{-1}). Therefore, portions of the outlet stream were analyzed (GC) at regular intervals (60 min) to determine the products distribution. While good levels of conversions (>50%) were detected at 30 °C with flow rates up to 30 μL min^{-1} (entries 1-4), full consumption of diketone **1a** was achieved with a flow rate of 5 μL min^{-1} (residence time: 56 min). Actually, driving the reaction to completion is an important goal in continuous process optimization for easier product purification; nevertheless, operation at the flow rate of 10 μL min^{-1} (residence time: 28 min) was considered the best compromise to provide a suitable balance between productivity (0.11 mmol d^{-1}) and conversion efficiency (78%, entry 2, Table 4). Therefore, the long-term stability of AAS-functionalized catalytic bed was next examined with 10 mM **1a** under the above continuous-flow conditions. As evidenced by Figure 5, the steady state-conversion was reached after *ca.* 1 h and maintained stable for 15 days on stream; significantly, 30 days operation determined a loss of only half the initial productivity.

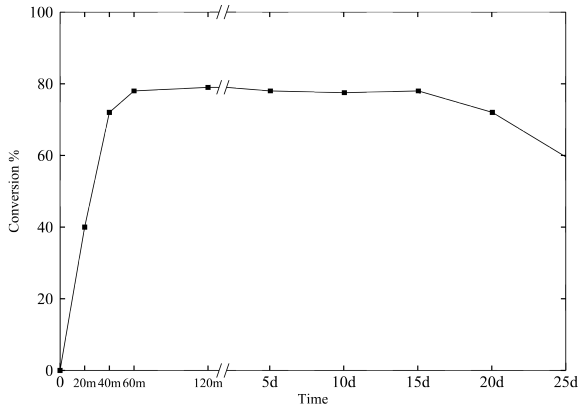

Figure 5. Conversion of continuous-flow **1a** homo-coupling as a function of time.

The scope and the applicability of the disclosed flow procedure were investigated by considering the homo-couplings of diketones **1b-g**. Gratifyingly, satisfactory conversion efficiencies (>50%) could be obtained by suitably adjusting the flow rate of the optimized feed solutions (entries 5-10). As previously observed for the tertiary alcohol **2a** (Table 4, entry 1), enantioselectivities of alcohols **2b-e** detected in batch experiments (Table 3) were replicated under flow conditions and maintained constant during the process in steady-state regime. Notably, the high selectivity of the flow procedure was confirmed by the unique formation of the target products **2** and **3** that are easily separable by chromatography and, in the case of incomplete conversions, by the recovery of unmodified starting diketone **1**. This result indicated that the acetyl anion

($MeCO^-$) transfer was predominant over migration of its higher carbanion counterparts under heterogeneous continuous-flow conditions as well. Moreover, in full agreement with AAS reactivity,[20a] the selectivity towards the formation of chiral alcohols **2** improved with the increase of steric hindrance of R^2 group, thus confirming the preferential attack of acetyl anion on the less bulky carbonyl carbon of the starting diketone **1** (Scheme 1).

Conclusions

In summary, we have initially described a method for the purification and immobilization on silica support of acetylacetoin synthase (AAS). Interest towards this not classical ThDP-dependent enzyme arises from its unique capability to furnish through the polarity reversal of α-diketones chiral tertiary alpha-hydroxyketones. These are densely functionalized derivatives containing a quaternary stereocenter of high synthetic utility and biological relevance. In preliminary batch experiments we have found that the immobilized AAS displayed a significantly enhanced stability compared to the free enzyme leading to high recyclability without loss of catalytic activity. Subsequently, the synthetic potential of AAS catalysis has been evaluated under flow conditions using fixed-bed microreactors fabricated with the silica-supported AAS as the packing material. Results from the continuous-flow set-up were fully consistent with those obtained from the batch process in terms of both conversion efficiency and stereoselectivity. Together with the ease of product/catalyst separation, a peculiar benefit of the flow-regime has been the remarkable long-term stability of the catalytic bed (more than 15 days on stream). While small-scale bioreactors have been presented in this study, an easy scale-up strategy may be envisaged through the use of multiple columns or the design of reactors with larger diameters. Therefore, we believe this work may represent a useful contribution to the current search for more efficient, economic, and environmentally benign production strategies of valuable chiral targets.

Experimental Section

All moisture-sensitive reactions were performed under a nitrogen atmosphere using oven-dried glassware. Solvents were dried over standard drying agent and freshly distilled prior to use. Reactions were monitored by TLC on silica gel 60 F_{254} with detection by charring with sulfuric acid and/or ninhydrin. Flash column chromatography was performed on silica gel 60 (230-400 mesh). Optical rotations were measured at 20 ± 2 °C in the stated solvent; $[a]_D$ values are given in 10^{-1} deg cm^2 g^{-1}. ^1H (300 MHz) and ^{13}C (75 MHz) NMR spectra were recorded for $CDCl_3$ solutions at room temperature unless otherwise specified. Peaks assignments were aided by ^1H-^1H COSY and gradient-HMQC experiments. Elemental analyses were performed with FLASH 2000 Series CHNS/O analyzer (ThermoFisher Scientific). Gas chromatographic analyses were performed on a Carlo Erba 6000, equipped with a FID detector and a fused capillary column Megadex 5 (25 m × 0.25 mm) containing dimethyl-*n*-pentyl-β-cyclodextrin on OV 1701 from Mega snc (temperature program from 80 to 200 °C with a gradient of 1.5 °C min^{-1} unless otherwise specified); helium was used as carrier gas (80 kPa). The mass spectra were obtained using a Varian 4000 GC/MS/MS equipped with chiral column Megadex 5, using the same conditions described for GC analyses. UV spectroscopic measurements were performed on Shimadzu UV-1601 UV-visible spectrophotometer. ESI MS (LTQ-XL Linear Trap from Thermo Scientific) analyses were performed in positive ion mode with samples dissolved in a 10 mM solution of HCO_2NH_4 in 1 : 1 MeCN–H_2O. Argonaut Technology. For accurate mass measurements, the compounds were analyzed in positive ion mode by Agilent 6520 HPLC-Chip Q/TOF-MS (nanospray) using a quadrupole, a hexapole, and a time-of-flight unit to produce spectra. The capillary source voltage was set at 1700V; the gas temperature and drying gas were kept at 350°C and 5 L/min, respectively. MS analyzer was externally calibrated with ESI-L low concentration tuning mix from *m/z* 118 to 2700 to yield accuracy below 5 ppm. Accurate mass data were collected by directly infusing samples in 40/60 H_2O/ACN 0.1% TFA into the system at a flow rate of 0.4 mL/min. Crude AAS was obtained from commercially available (DSMZ) *B. licheniformis* DSM13 as described.[18] Spherical silica gel (Microsorb 300-5 Si, particle size 5 μm, pore size 300 Å) was purchased from Varian. Diketones **1a**, **1b**, **1c**, **1e**, **1f**, and **1g** are commercially available from Sigma-Aldrich. Diketone **1d** was synthesized as described.[20b]

Preparation of 3-aminopropyl silica gel

To preserve spherical shape of silica particles, this derivatization step was carried out in a standard rotary evaporator in which a two-necked flask was fitted with solvent condenser, solvent collector, and nitrogen inlet for syringe addition of reactant solutions under an inert atmosphere. Mixing was obtained by spinning the flask around its axis and warming by means of a standard oil-bath. Microsorb 300-5 Si silica gel was dried before its use (0.1 mbar, T= 110 °C, 2 h).

To a stirred slurry of Microsorb 300-5 Si (5.00 g), anhydrous toluene (60 mL), and freshly distilled triethylamine (0.25 mL) was slowly added a solution of (3-aminopropyl)-trimethoxysilane (4 mL) in anhydrous toluene (10 mL). The resulting mixture was then warmed to 60 °C and stirred for 20 h. Subsequently, the mixture was refluxed until ca. 15 mL of solvent were collected (eventually by the aid of a nitrogen stream). The mixture was then refluxed for an additional hour, cooled to room temperature, and centrifuged with 20-mL portions of toluene, MeOH, EtOH, and cyclohexane. The resulting 3-aminopropyl silica gel was finally dried at reduced pressure (0.1 mbar, 60 °C, 6 h). Elemental analysis (%) found: N 0.45 (estimated loading f = 0.32 $mmolg^{-1}$).

Acetylacetoin synthase (AAS) production and purification

The cells of *B. licheniformis* DSM13 were cultured and treated as described[18] in order to obtain the cell free extract that represents the starting material of the following purification procedure. The purification of the enzyme was checked by measuring the activity as reported below and determining the protein concentration through spectrophotometric measurements at 215 and 280 nm.[30] The extract (26 mL) was fractionated with ammonium sulfate and the proteins precipitated between 40 and 60% saturation were collected by centrifugation (6000 rpm, 15 min, r.t.). The pellet was dissolved in phosphate buffer 50 mM, pH 7 (5 mL) and desalted by repeated ultrafiltration (Amicon Ultra-4 membrane). The desalted protein solution (6 mL, 1.8 U) was loaded on a DEAE-Sepharose column (length 3.0 cm, diameter 1.5 cm), equilibrated with phosphate buffer 50 mM (pH 7), and eluted with a step-gradient of NaCl in the equilibration buffer (0.2, 0.4

and 0.6 M). The fractions were assayed for determining the enzyme activity and protein concentration; the active fractions eluted with 0.4 M NaCl were pooled (10 mL, 1.2 U). This enzyme solution was treated with ammonium sulfate (80% of the saturating concentration) in order to precipitate the partially purified AAS that, in this form can be stored at 4 °C for at least two months without significant loss of activity.

Enzyme assay

The enzyme solution (50-100 μL) was added to a reaction mixture (1 mL) containing 2,3-pentanedione **1a** (10 mM), ThDP (0.4 mM), and $MgSO_4$ (0.8 mM) dissolved in phosphate buffer 50 mM (pH 6.5). The reaction mixture was gently shaken at 30 °C and samples (0.15 mL) were withdrawn after 30, 60 and 120 min. The samples were extracted with AcOEt (0.2 mL) containing diethyl carbonate (0.05%) as internal standard and the organic extracts were subjected to chiral GC analysis.[20a] One unit (U) of AAS was defined as the amount catalyzing the formation of 1 μmol of the mixture of products **2a** and **3a** (for the ratio see Table 3) in one minute.

AAS immobilization: optimization of pH

3-Aminopropyl silica gel (30 mg) was suspended in 50 mM phosphate buffer (pH 7, 1 mL), then a 25% aqueous solution glutaraldehyde (0.1 mL) was added in one portion. After shaking for 2 h at 30 °C silica was filtered and washed with water. The carrier was suspended in water (1 mL) and the resulting suspension divided into four equivalent portions. After centrifugation (3.000 rpm, 3 min) the supernatant was discharged and to each pellet a solution of the partially purified AAS (0.8 mg, 0.08 U) in different buffers (1 mL) was added. For pH 5, acetate 50 mM was used as buffering agent while for pH 6, 7 and 8 phosphate 50 mM was employed. The suspensions were shaken at 25 °C for 2h and then centrifuged and each pellet was washed with phosphate 50 mM at pH 7 (3 × 1 mL). The amount of immobilized proteins (see Figure 3) were determined from the difference between the protein concentration of the supernatant before and after the immobilization, whereas the enzymatic activity of the solutions and pellets were determined as described before.

AAS immobilization: optimization of the enzyme/carrier ratio (w/w)

3-Aminopropyl silica gel (25 mg) was suspended in phosphate buffer (pH 7, 1 mL) and treated with the glutaraldehyde solution as described in the previous paragraph. Five equivalent portions of the resulting silica (5 mg) were suspended in 50 mM phosphate buffer at pH 6 (1 mL) containing different amounts of partially purified AAS (0.125, 0.25, 0.5, 1, and 2 mg). The suspensions were shaken at 25 °C for 2.5 h and then centrifuged. The amount of immobilized proteins and the activity of the carrier bound enzyme (Table 2) were determined as described before.

AAS immobilization: effect of the Schiff's base double bonds reduction

The immobilized AAS (20 mg) prepared as described in the previous paragraph (enzyme/carrier ratio 0.2:1) was suspended in phosphate buffer 50 mM at pH 6.5 (4 mL). The suspension was divided into two equivalent portions; the first one was used for a control experiment. To the second one sodium cyanoborohydride (13 mg, 0.20 mmol) was added in small portions. The two samples were shaken at 25 °C for 1.5 hours and then washed with the above buffer. The activity of the two heterogeneous catalysts were assayed by GC-analysis showing a volumetric activity of 3.5 and 0.8 U g^{-1} for the reference and reduced catalyst, respectively. The assays were daily repeated for one month: final volumetric activities of 2.8 and 0.6 U g^{-1}.

Effect of pH on the activity of free and immobilized AAS

The free and the immobilized AAS enzyme (*ca.* 0.01 U) were added to a reaction mixture (1 mL) containing 2,3-pentanedione **1a** (10 mM), ThDP (0.4 mM) and $MgSO_4$ (0.8 mM) dissolved in the proper buffer. The used buffers were 50 mM acetate for pH 5 and 50 mM phosphate for pH 6-8. After 2 h the reactions were treated and analyzed as described before. The results are summarized in Figure 4.

Homo-coupling of α-diketones 1a-g with immobilized AAS under batch conditions

The heterogeneous enzyme prepared under the above optimized immobilization conditions (pH 6.0, enzyme/carrier ratio = 0.2:1, no imine bonds reduction) was used in this study. The silica supported AAS (250 mg, *ca.* 0.9 U) was added to a solution of ThDP (18 mg, 0.04 mmol), $MgSO_4$ (10 mg, 0.08 mmol) in phosphate buffer 50 mM at pH 6.5 (100 mL). The α-diketone **1** (1 mmol) dissolved in DMSO (1 mL) was then added to the above suspension; the reaction was performed in a reciprocal shaker (100 rpm) at 30 °C for 10 h. After removing the catalyst by filtration, the aqueous mixture was extracted with Et_2O (3 × 20 mL) and the combined organic layers were washed with a saturated NaH_2CO_3 solution (5 mL). The ethereal solvent was then removed under a nitrogen stream and the residue containing the target α-hydroxyketones **2** and **3** purified by either bulb-to-bulb distillation (compounds **3f** and **3g**) or flash chromatography (compounds **2a-d** and **3a-d**).

(*R*)-3-Hydroxy-3-methylhexane-2,4-dione (2a). Column chromatography with 12:1 cyclohexane-AcOEt afforded **2a**[20a] (66 mg, 46%) as a colorless oil; $[\alpha]_D$= 18.2 (*c* 0.5, $CHCl_3$). ^{1}H NMR: δ = 1.05 (t, 3 H, *J* = 7.5 Hz, CH_3), 1.55 (s, 3 H, CH_3), 2.27 (s, 3 H, CH_3CO), 2.51 (dq, 1 H, *J* = 21 Hz, *J* = 7.5 Hz, CH_{2a}), 2.73 (dq, 1 H, *J* = 21 Hz, *J* =7.5 Hz, CH_{2b}), 4.65 (br s, 1 H, OH); ^{13}C NMR: δ = 7.5, 22.8, 24.5, 87.4, 207.4, 210.2; GC–MS: retention time: 15.4 (*S*)-enantiomer and 15.9 (*R*)-enantiomer, ee 85%; MS (70eV, EI); *m/z* (%) 145 (≤1), 102 (27), 88 (100), 57 (25), 43 (30). ESI MS (144.1): 145.1 (M + H^+). HRMS (ESI) *m/z* calcd for $C_7H_{13}O_3$ [M + H]$^+$ 145.0845, found 145.0892. Found: C, 58.55; H, 8.21. $C_7H_{12}O_3$ requires C, 58.32; H, 8.39%.

A chromatographic fraction containing 3-ethyl-3-hydroxy-2,4-pentanedione **3a** was collected for **3a**[20a] identification. Compound **3a** partially decomposes on silica gel. ^{1}H NMR: δ = 1.85 (t, 3 H, *J* = 7.5 Hz, CH_3), 2.05 (q, 2 H, *J* = 7.5 Hz, CH_2), 2.27 (s, 6 H, 2 CH_3CO); 4.7 (br s, 1 H, OH).

(*R*)-3-Hydroxy-3-methyl-2,4-heptanedione (2b). Column chromatography with 12:1 cyclohexane-AcOEt afforded **2b**[20a] (76 mg, 48%) as a colorless oil; $[\alpha]_D$= 4.1 (*c* 0.5, $CHCl_3$). ^{1}H NMR: δ = 0.91 (t, 3 H, *J* = 7.5 Hz, CH_3), 1.56 (s, 3 H, CH_3), 1.58–1.65 (m, 2 H, CH_2), 2.25 (s, 3 H, CH_3CO), 2.49 (dt, 1 H, *J* = 17.5 Hz, *J* = 7.5 Hz, CH_{2a}), 2.68 (dt, 1 H, *J* = 17.5 Hz, *J* = 7.5 Hz CH_{2b}), 4.75 (br s, 1 H, OH); ^{13}C NMR: δ = 13.5, 16.8, 22.6, 24.6, 38.6, 87.6, 207.4, 209.5; GC–MS: retention time (min) 20.8 (*S*)-enantiomer and 20.9 (*R*)-enantiomer, ee 91%; MS (70 eV, EI): *m/z* (%) 159 (≤1), 116 (21), 88 (100), 71 (37), 43 (46). ESI MS (158.2): 181.4 (M + Na^+). HRMS (ESI) *m/z* calcd for

$C_8H_{14}O_3$ $[M]^+$ 158.0943, found 158.0912. Found: C, 60.98; H, 8.70. $C_8H_{14}O_3$ requires C, 60.74; H, 8.92%.
A chromatographic fraction containing 3-hydroxy-3-propylpentane-2,4-dione **3b** was collected for **3b**[20a] identification. Compound **3b** partially decomposes on silica gel. ^{1}H NMR: δ = 0.95 (t, 3 H, *J* = 7.5 Hz, CH_3); 1.22 (m, 2 H, C*H*$_2$); 1.93 (m, 2 H, C*H*$_2$), 2.24 (s, 6 H, 2 CH_3CO), 4.65 (br s, 1 H, OH).

(*R*)-3-Hydroxy-3-methyl-2,4-octanedione (2c). Column chromatography with 12:1 cyclohexane-AcOEt afforded **2c**[18] (77 mg, 45%) as a colorless oil; $[\alpha]_D$= 7.3 (*c* 0.2, $CHCl_3$). ^{1}H NMR: δ = 0.93 (t, 3 H, *J* = 7.5 Hz, CH_3) 1.22–1.36 (m, 2 H, CH_2) 1.48–1.62 (m, 2 H, CH_2) 1.56 (s, 3 H, CH_3) 2.25 (s, 3 H, CH_3CO) 2.51 (dt, 1 H, *J* = 17.5 Hz, *J* = 7.5 Hz, CH_2CO) 2.70 (dt, 1 H, *J* = 17.5, *J* = 7.5 Hz CH_2CO) 4.75 (br s, 1 H, OH). ^{13}C NMR: δ = 13.8, 22.5, 22,7, 24.6, 25.5, 36.5, 87.6, 207.4, 209.6; GC–MS: retention time (min) 23.7 (*S*)-enantiomer and 23.8 (*R*)-enantiomer, ee 72%; MS (70 eV, EI): *m/z* (%) 172 (<1), 130 (20), 88 (100), 43 (45). ESI MS (172.2): 173.8 (M + H^+). HRMS (ESI) *m/z* calcd for $C_9H_{17}O_3$ $[M + H]^+$ 173.1178, found 173.1112. Found: C, 62.88; H, 9.12. $C_9H_{16}O_3$ requires C, 62.77; H, 9.36%.
A chromatographic fraction containing 3-butyl-3-hydroxypentane-2,4-dione **3c**[18] was collected for **3c** identification. Compound **3c** partially decomposes on silica gel. ^{1}H NMR: δ = 0.91 (t, 3 H, *J* = 7.5 Hz, CH_3) 1.10–1.40 (m, 4 H, 2 CH_2), 1.95–2.05 (m, 2 H, CH_2) 2.25 (s, 6 H, 2 CH_3CO) 4.65 (br s, 1 H, OH).

(*R*)-3-Hydroxy-3-methylnonane-2,4-dione (2d). Column chromatography with 20:1 cyclohexane-AcOEt afforded **2d**[20b] (108 mg, 58%) as a colorless oil; $[\alpha]_D$= 10.4 (*c* 0.2, $CHCl_3$). ^{1}H NMR: δ = 0.85 (t, *J* = 7.5 Hz, 3 H, CH_3), 1.15–1.35 (m, 5 H), 1.52 (s, 3 H), 1.45–1.58 (m, 1 H), 2.20 (s, 3 H), 2.47 (dt, *J* = 7.0 Hz, *J* = 17.0 Hz, 1 H), 2.65 (dt, *J* = 7.0Hz, *J* = 17.0 Hz, 1 H), 4.70 (s, 1 H); ^{13}C NMR: δ = 13.8, 22.3, 22.6, 22.7, 23.0, 31.1, 36.7, 87.5, 207.4, 209.6; GC–MS: retention time (min) 22.7 (*S*)-enantiomer and 22.9 (*R*)-enantiomer, ee 55%; MS (70 eV, EI): *m/z* (%) 187 (3), 144 (20), 99 (55), 88 (100). ESI MS (186.2): 187.7 (M + H^+). HRMS (ESI) *m/z* calcd for $C_{10}H_{18}NaO_3$ $[M + Na]^+$ 209.1154, found 209.1180. Found: C, 64.88; H, 9.52. $C_{10}H_{18}O_3$ requires C, 64.49; H, 9.74%.
A chromatographic fraction containing 3-butyl-3-hydroxypentane-2,4-dione **3d**[20b] was collected for **3d** identification. ^{1}H NMR: δ = 0.92 (t, *J* = 7.0 Hz, 3 H), 1.20 (m, 6 H), 1.95–2.05 (m, 2 H), 2.28 (s, 6 H), 4.70 (s, 1 H).

(*R*)-2-Hydroxy-2-methyl-1-phenyl-1,3-butanedione (2e). Column chromatography with 10:1 cyclohexane-AcOEt afforded **2e**[20a] (67 mg, 35%) as a colorless oil; $[\alpha]_D$= 13.7 (*c* 0.5, $CHCl_3$). ^{1}H NMR: δ = 1.70 (s, 3H, CH_3), 2.24 (s, 3 H, CH_3CO), 5.02 (br s, 1 H, OH), 7.42–8.21 (m, 5 H, Ph); ^{13}C NMR: δ = 23.4, 24.7, 85.8, 128.6, 129.8, 133.6, 133.9, 197.9, 206.5; GC–MS (temperature program from 100 to 200 °C with a gradient of 5 °C min^{-1}): retention time (min) 16.6 (*S*)-enantiomer and 16.7 (*S*)-enantiomer, ee 80%; MS (70 eV, EI): *m/z* (%) 193 (2), 150 (24), 105 (100), 77 (56). ESI MS (192.2): 215.8 (M + Na^+). HRMS (ESI) *m/z* calcd for $C_{11}H_{12}O_3$ $[M]^+$ 192.0786, found 192.0755. Found: C, 68.22; H, 6.45. $C_{11}H_{12}O_3$ requires C, 68.74; H, 6.29%.

3-Hydroxy-3-methylpentane-2,4-dione (3f). The crude reaction mixture was bulb-to-bulb distilled (50 °C, 5 mmHg) to give **3f**[20a,30] (111 mg, 85%) as a colorless liquid. Lit.:[30] bp 43-44 °C (4 mmHg). ^{1}H NMR: δ = 1.60 (s, 3 H, CH_3), 2.30 (s, 6 H, 2 CH_3CO), 4.70 (s, 1 H, OH). ^{13}C NMR: δ = 22.6, 24.7, 87.6, 207.4; GC–MS (temperature program from 60 to 200 °C with a gradient of 2 °C min^{-1}): retention time (min) 15.1. ESI MS (130.1): 153.4 (M + Na^+). HRMS (ESI) *m/z* calcd for $C_6H_{10}NaO_3$ $[M+ Na]^+$ 153.0528, found 153.0562. Found: C, 55.20; H, 7.88. $C_6H_{10}O_3$ requires C, 55.37; H, 7.74%. Compound **3f** partially decomposes on silica gel.

4-Ethyl-4-hydroxyheptane-3,5-dione (3g). The crude reaction mixture was bulb-to-bulb distilled (84 °C, 5 mmHg) to give **3g**[20a,32] (134 mg, 78%) as a colorless liquid. ^{1}H NMR: δ = 0.82 (t, 3 H, *J* = 7.5 Hz, CH_3), 1.04 (t, 6 H, *J* = 7.5 Hz, 2 CH_3), 2.04 (q, 2 H, *J* = 7.5 Hz, CH_2), 2.51 (dq, 2 H, *J* = 21.0 Hz, *J* = 7.5 Hz, C*H*$_2$), 2.73 (dq, 2 H, *J* = 21.0 Hz, *J* = 7.5 Hz, C*H*$_2$), 4.65 (br s, 1 H, OH); ^{13}C NMR: δ = 7.3, 7.4, 29.8, 30.6, 90.9, 210.2; GC–MS: retention time (min) 22.5. ESI MS (172.2): 173.5 (M + H^+). HRMS (ESI) *m/z* calcd for $C_9H_{16}O_3$ $[M]^+$ 172.1099, found 172.1028. Found: C, 55.20; H, 7.88. $C_9H_{16}O_3$ requires C, 62.77; H, 9.36%. Compound **3g** partially decomposes on silica gel.

Microreactor preparation/characterization and instrumental set-up
Microreactor packing. The microreactor was fabricated by using a 100 × 2.1 mm stainless steel column, which was filled with 3-aminopropyl silica by slurry-packing. Slurry-packing was performed under constant pressure (300 bars, 30 min, toluene as solvent) by using an air driven liquid pump (by Haskel). Slurry was prepared by suspending excess in weight of functionalized silica in toluene.
Determination of microreactor void-volume. Microreactor void volume (V_0) was determined by pycnometry.[33] This method consists in filling the microreactor successively with two distinct solvents (here noted as 1 and 2) and weighing the filled microreactors accurately. Simple math shows that:[34]

$$V_0 = \frac{w_1 - w_2}{\delta_1 - \delta_2} \quad (1)$$

where ω_1 and ω_2 are the weights of the microreactor filled with solvents 1 and 2 and δ_1 and δ_2 the densities of the solvents.
Determination of packing amount inside the microreactor. The determination of the amount of material contained in the microreactor is based on the consideration that the microreactor weight, ω_{tot}, can be expressed as:

$$w_{tot} = w_0 + w_{ads} + w_{hw} \quad (2)$$

where ω_0 and ω_{ads} are the weight of the liquid and that of the adsorbent inside the reactor (packing), respectively. ω_{hw} is the weight of the stainless steel hardware (i.e., the weight of the empty microreactor). Eq. 2 can be rewritten as:

$$w_{tot} = V_0\delta_0 + w_{ads} + w_{hw} \quad (3)$$

where δ_0 is the density of the solvent with which the microreactor was filled. Since V_0 is known from Eq. 1, ω_{tot} is readily available and ω_{hw} can be measured before packing, Eq. 3 permits the estimation of ω_{ads} for a slurry-packed microreactor without destroying the device.

Enzyme immobilization under flow conditions
The microreactor was provided with fittings, connected to an HPLC pump, and washed in sequence with isopropanol, water, and 50 mM phosphate buffer at pH 7. After that, a 2.5% glutaraldehyde solution in 50 mM phosphate buffer at pH 7 was

flushed through the column (2 h; flow rate: 0.15 mL/min) and then washed with 50 mM phosphate buffer at pH 6 (2 h; flow rate: 0.15 mL/min). The aldehyde functionalized column was then fed (flow rate: 0.10 mL/min) with a 0.1% (w/v) solution of AAS in phosphate buffer pH 6 (20 mL) containing ThDP (0.4 mM) and $MgSO_4$ (0.8 mM). The resulting bioreactor was finally washed with the buffer until the eluate absorbance at 280 nm reached the background value.

Homo-coupling of α-diketones 1a-g under flow conditions

The microreactor was equilibrated with triethanolamine 50 mM at pH 6.5 and then fed with a solution of α-diketone **1** (10 mM; see Table 4 for different molarity concentrations), ThDP (0.04 mM) and $MgSO_4$ (0.08 mM) in the equilibration buffer containing DMSO (1% w/v). The microreactor was operated at 30 °C for 24 h (under steady-state conditions) at the stated flow rate. Instant conversion was determined (GC analysis) every 60 min by taking a sample of the eluate. The solution collected after 24 h was extracted with Et_2O (3 × 20 mL) and the combined organic layers were washed with a saturated NaH_2CO_3 solution (5 mL). The ethereal solvent was then removed under a nitrogen stream and the residue containing the target α-hydroxyketones **2** and **3** purified by either bulb-to-bulb distillation (compounds **3f** and **3g**) or flash chromatography (compounds **2a-d** and **3a-d**).

The long-term stability experiment was performed using α-diketone **1** (0.10 M) as the substrate; the microreactor was operated at 30 °C with a flow rate of 10 μL min^{-1} for 30 days. After the achievement of the steady-state regime (ca. 1 h), conversion of **1a** in the range 78-70 % was maintained for 15 days, while a progressive loss of catalytic activity was observed after that time.

Acknowledgements

We gratefully acknowledge University of Ferrara (fondi FAR) for financial support. Thanks are also given to Mr. P. Formaglio for NMR spectroscopic experiments, to Mrs. E. Bianchini for elemental analyses, to Dr. T. Bernardi for high-resolution mass spectrometric experiments, and to Dr. M. De Bastiani for electrophoretic analyses.

Notes and references

[a] *Dipartimento di Scienze Chimiche e Farmaceutiche, Università di Ferrara, Via Fossato di Mortara 17, I-44121 Ferrara (Italy). E-mail:* pierpaolo.giovannini@unife.it - alessandro.massi@unife.it

1 (*a*) T. Tsubogo, T. Ishiwata and S. Kobayashi, *Angew. Chem., Int. Ed.,* 2013, **52**, 6590; (*b*) A. Puglisi, M. Benaglia and V. Chiroli, *Green Chem*., 2013, **15**, 1790; (*c*) T. Chinnusamy, S. Yudha S , M. Hager, P. Kreitmeier and O. Reiser, *ChemSusChem*, 2012, **5**, 247; (*d*) D. Zhao and K. Ding, *ACS Catal.*, 2013, **3**, 928; (*e*) X. Y. Mak, P. Laurino and P. H. Seeberger, *Beilstein J. Org. Chem.*, 2009, **5**, DOI: 10.3762/bjoc.5.19.

2. (*a*) V. Hessel, D. Kralisch, N. Kockmann, T. Noël and Q. Wang, *ChemSusChem*, 2013, **6**, 746; (*b*) S. C. Stouten, T. Noël, Q. Wang and V. Hessel, *Aust. J. Chem.*, 2013, **66**, 121; (*c*) D. T. McQuade and P. H. Seeberger, *J. Org. Chem*., 2103, *78*, 6384; (*d*) T. Illg, P. Löb and V. Hessel, *Bioorg. Med. Chem.*, 2010, **18**, 3707; (*e*) K. Geyer, T. Gustafsson and P. H. Seeberger, *Synlett*, 2009, 2382; (*f*) B. P. Mason, K. E. Price, J. L. Steinbacher, A. R. Bogdan and D. T. McQuade, *Chem. Rev.,* 2007, **107**, 2300; (*g*) I. R. Baxendale, S. V. Ley, A. C. Mansfield and C. D. Smith, *Angew. Chem., Int. Ed.,* 2009, *48*, 4017; (*h*) I. R. Baxendale, J. J. Hayward, S. Lanners, S. V. Ley and C. D. Smith, in *Microreactors in Organic Synthesis and Catalysis*, ed. T. Wirth, Wiley-VCH, Weinheim, 2008, ch. 4.2, pp. 84; (*i*) A. R. Bogdan, S. L. Poe, D. C. Kubis, S. J. Broadwater and D. T. McQuade, *Angew. Chem., Int. Ed*., 2009, **48**, 8547; (*j*) F. E. Valera, M. Quaranta, A. Moran, J. Blacker, A. Armstrong, J. T. Cabral and D. G. Blackmond, *Angew. Chem., Int. Ed.*, 2010, **49**, 2478; (*k*) L. Malet-Sanz and F. Susanne, *J. Med. Chem.,* 2012, **5**5, 4062.

3. (*a*) C. G. Frost and L. Mutton, *Green Chem.*, 2010, **12**, 1687; (*b*) A. R. Bogdan, B. P. Mason, K. T. Sylvester and D. T. McQuade, *Angew. Chem., Int. Ed*., 2007, **46**, 1698; (*c*) A. Kirschning, W. Solodenko and K. Mennecke, *Chem.–Eur. J.,* 2006, **12**, 5972; (*d*) M. Irfan, T. N. Glasnov and C. Oliver Kappe, *ChemSusChem*, 2011, **4**, 300.

4. (*a*) O. Bortolini, A. Cavazzini, P. Dambruoso, P. P. Giovannini, L. Caciolli, A. Massi, S. Pacifico and Daniele Ragno, *Green Chem*., 2013, **15**, 2981; (*b*) O. Bortolini, A. Cavazzini, P. P. Giovannini, R. Greco, N. Marchetti, A. Massi and L. Pasti, *Chem.–Eur. J*., 2013, **19**, 7802; (*c*) O. Bortolini, L. Caciolli, A. Cavazzini, V. Costa, R. Greco, A. Massi and L. Pasti, *Green Chem.*, 2012, **14**, 992; (*d*) A. Massi, A. Cavazzini, L. Del Zoppo, O. Pandoli, V. Costa, L. Pasti and P. P. Giovannini, *Tetrahedron Lett.,* 2011, **52**, 619; (*e*) A. Massi, O. Pandoli, A. Cavazzini, L. Del Zoppo, P. P. Giovannini and C. Bendazzoli, *Italian Patent*, No. 0001398243, 2013.

5. (*a*) G. Kardos and T. Soós, *Eur. J. Org. Chem*., 2013, 4490; (*b*) P. Kasaplar, C. Rodríguez-Escrich and M. A. Pericàs, *Org. Lett.*, 2013, **15**, 3498; (*c*) Y. Arakawa and H. Wennemers, *ChemSusChem*, 2013, **6**, 242; (*d*) S. B. Otvos, I. M. Mandity and F. Fulop, *ChemSusChem*, 2012, **5**, 266; (*e*) L. Osorio-Planes, C. Rodríguez-Escrich and M. A. Pericàs, *Org. Lett.*, 2012, **14**, 1816; (*f*) C. Ayats, A. H. Henseler and M. A. Pericàs, *ChemSusChem*, 2012, **5**, 320; (*g*) X. C. Cambeiro, R. Martín-Rapún, P. O. Miranda, S. Sayalero, E. Alza, P. Llanes and M. A. Pericàs, *Beilstein J. Org. Chem*., 2011, **7**, 1486; (*h*) A. L. W. Demuynck, L. Peng, F. de Clippel and J. Vanderleyden, *Adv. Synth. Catal.*, 2011, **353**, 725; (*i*) E. Alza, S. Sayalero, X. C. Cambeiro, R. Martín-Rapún, P. O. Miranda and M. A. Pericàs, *Synlett*, 2011, 464; (*j*) E. Alza, C. Rodríguez-Escrich, S. Sayalero, A. Bastero and M. A. Pericàs, *Chem.–Eur. J.*, 2009, **15**, 10167; (*k*) F. Bonfils, I. Cazaux, P. Hodge and C. Caze, *Org. Biomol. Chem*., 2006, **4**, 493; (*l*) D. Bernstein, S. France, J. Wolfer and T. Lectka, *Tetrahedron: Asymmetry*, 2005, **16**, 3481; (*m*) S. France, D. Bernstein, A. Weatherwax and T. Lectka, *Org. Lett.*, 2005, **7**, 3009; (*n*) A. M. Hafez, A. E. Taggi, T. Dudding and T. Lectka, *J. Am. Chem. Soc.*, 2001, **123**, 18853; (*o*) R. Porta, M. Benaglia, V. Chiroli, F. Coccia and Alessandra Puglisi, *Israel J. Chem.*, 2014, DOI: 10.1002/ijch.201300106; (*p*) S. Martín, R. Porcar, E. Peris, M. I. Burguete, E. García-Verdugo and S. V. Luis, *Green Chem*., 2014, **16**, 1639; (*q*) V. Chiroli, M. Benaglia, A. Puglisi, R. Porta, R. P. Jumde and A. Mandoli, *Green Chem.*, 2014, **16**, 2798; (*r*) R. Martín-Rapún, S. Sayalero and M. A. Pericàs, *Green Chem.*, 2013, **15**, 3295; (*s*) V. Chiroli, M. Benaglia, F. Cozzi, A. Puglisi, R. Annunziata and G. Celentano, *Org. Lett.*, 2013, **15**, 3590; (*t*) M. Rueping, C. Vila and T. Bootwicha, *ACS Catal*., 2013, **3**, 1676; (*u*) E. Sugiono and M. Rueping, *Beilstein J. Org. Chem.,* 2013, **9**, 2457.

6. M. Movassaghi and E. N. Jacobsen, *Science*, 2002, **298**, 1904.

7. (*a*) A. Liese, K. Seebach and C. Wandrey, *Industrial Biotransformations*, 2nd ed., Wiley-VCH, Weinheim, 2006; (*b*) N. N. Rao, S. Lütz, K. Wurges and D. Minör, *Org. Process Res. Dev.,* 2009, **13**, 607; (*c*) G. Grogan, *Annu. Rep. Progr. Chem., Sect. B: Org. Chem.,* **2013**, *109,* 15; (*d*) N. End and U. Schöning, *Top. Curr. Chem.*, 2004, **242**, 273.
8. (*a*) H. E. Schoemaker, D. Mink, M. G. Wubbolts, *Science* 2003, **299**, 1694; (*b*) U. T. Bornscheuer, G. W. Huisman, R. J. Kazlauskas, S. Lutz, J. C. Moore and K. Robins, *Nature*, 2012, **485**, 185.
9. (*a*) P. Rasor, *Immobilized enzymes in enantioselective organic synthesis in Chiral catalyst immobilization and recycling*, eds. D. E. De Vos, I. F. J. Vancelecom and P. A. Jacobs, Wiley-VCH, Weinheim, 2000, pp. 97; (*b*) G.F. Bickerstaff, *Immobilization of biocatalysts in molecular biology and biotechnology*, eds. J. M. Walker and R. Rapley, RCS, London, 4th ed., 2000, pp. 433; (*c*) L. Lalonde and A. Margolin, in *Enzyme catalysis in organic synthesis*, Vol. 1, eds. K. Drauz and H. Waldmann, Wiley-VCH, Weinheim, 2nd revised ed., Vol. 1, 2002, pp. 163; (*d*) S. Pedersen and M. W. Christensen, in *Applied Biocatalysis,* eds. A. J. J. Straathof and P. Adlercreutz, CRC Press, Boca Raton, 2nd ed., 2000, p. 213.
10. (*a*) K. Faber and R. Patel, *Curr. Opin. Biotechnol.,* 2000, **11**, 517; (*b*) W. Keim and B. Driessen-Holscher, *Supported catalysts. Deposition of active component. Heterogenization of complexes and enzymes in Preparation of solid catalysts*, eds.: G. K. H. Ertl and J. Weitkamp, Wiley-VCH, Weinheim, 1999, pp. 355.
11. (*a*) I. J. Dunn, E. Heinzle, J. Ingham and J. E. Prenosil, *Biological Reaction Engineering*, Wiley-VCH, Weinheim, 2003; (*b*) E. G. Vlakh and T. B. Tennikova, *J. Sep. Sci.,* 2013, **36***,* 110; (*c*) E. G. Vlakh and T. B. Tennikova, *J. Sep. Sci.,* 2013, **36***,* 1149.
12. (*a*) I. Itabaiana Jr., L. S. de Mariz e Miranda and R. O. M. Alves de Souza, *J. Mol. Catal. B: Enzym.,* 2013, **85-86,** 1; (*b*) R. Yuryev, S. Strompen and Andreas Liese, *Beilstein J. Org. Chem.,* 2011, **7**, 1449; (*c*) Z. Liu, J. Zhang, X. Chen, P.G. Wang, *ChemBioChem*, 2002, **3**, 348; (*d*) M. J. Fink, M. Scöhn, F. Rudroff, M. Schnürch and M. D. Mihovilovic, *ChemCatChem*, 2013, **5**, 724.
13. (*a*) P. Fernandes, *Int. J. Mol. Sci.,* **2010**, *11,* 858; (*b*) M. S. Thomsen and B. Nidetzky, *Eng. Life Sci.,* 2008, **8**, 40; (*c*) J. M. Bolivar, J. Wiesbauer and B Nidetzky, *Trends Biotechnol*., 2011, **29**, 333; (*d*) M. Wu, H. Zhang, Z. Wang, S. Shen, X. C. Lea and X.-F. Li, *Chem. Commun.,* 2013, **49**, 1407; (*e*) R. de Oliveira Lopes, A. S. de Miranda, B. Reichart, T. Glasnov, C. O. Kappe, R. C. Simon, W. Kroutil, L. S. M. Miranda, I. C. R. Leal, R. O. M. A. de Souza, *J. Mol. Catal. B: Enzym.*, 2014, **104**, 107. For an interesting study on enzyme-catalyzed ring-opening polymerization in microreactors, see: (*f*) S. Kundu, A. S. Bhangale, W. E. Wallace, K. M. Flynn, C. M. Guttman, R. A. Gross and K. L. Beers, *J. Am. Chem. Soc.*, 2011, **133**, 6006.
14. (*a*) P. Chen, S. Han, G. Lin and Z. Li, *J. Org. Chem*., 2002, **67**, 8251; (*b*) K. Koch, R. J. F. van den Berg, P. J. Nieuwland, R. Wijtmans, H. E. Schoemaker, J. C. M. van Hest and F. P. J. T. Rutjes, *Biotechnol. Bioeng.,* 2007, **99**, 1028.
15. L. Babich, A. F. Hartog, L. J. C. van Hemert, F. P. J. T. Rutjes and R. Wever, *ChemSusChem*, 2012, **5**, 2348.
16. (*a*) G. Dräger, C. Kiss, U. Kunz and A. Kirschning, *Org. Biomol. Chem.,* 2007, **5**, 3657; (*b*) N. Kurlemann and A. Liese, *Tetrahedron: Asymmetry*, 2004, **15**, 2955; (*c*) H. S. Shin and P. L. Rogers, *Biotechnol. Bioeng*., 1996, **49**, 429; (*d*) F. Hildebrand, S. Khül, M. Pohl, D. Vasic-Racki, M. Müller, C. Wandrey and S. Lütz, *Biotechnol. Bioeng*., 2006, **96**, 835; (*e*) R. Mikolajek, A. C. Spiess, M. Pohl, S. Lamare and J. Büchs, *ChemBioChem*, 2007, **8**, 1063; (*f*) T. Stillger, M. Pohl, C. Wandrey and A. Liese, *Org. Process Res. Dev.,* 2006, **10**, 1172; (*g*) A. A. Halima, N. Szitaa, F. Baganz, *J. Biotechnol.*, 2013, **168**, 567; (*h*) J. Lawrence, B. O'Sullivan, G. J. Lye, R. Wohlgemuth and N. Szitaa, *J. Mol. Catal. B: Enzym.,* 2013, **95**, 111; (*i*) B. O'Sullivan, H. Al-Bahrani, J. Lawrence, M. Campos, A. Cázares, F. Baganz, R. Wohlgemuth, H. C. Hailes and N. Szita, *J. Mol. Catal. B: Enzym.,* 2012, **77**, 1.
17. (*a*) G. Olack and H. Morrison, *J. Org. Chem.,* 1991, **56**, 4969; (*b*) F. A. Davis, C. Clark, A. Kumar and B.-C. Chen, *J. Org. Chem.,* 1994, **59**, 1184; (*c*) K. Tamaki, J. B. Shotwell, R. D. White, I. Drutu, D. T. Petsch, T. V. Nheu, H. He, Y. Hirokawa, H. Maruta and J. L. Wood, *Org. Lett*., 2001, **3**, 1689; (*d*) F. Neuser, H. Zorn and R. G. Berger, *J. Agric. Food Chem*., 2000, **48**, 6191; (*e*) P. E. Sum and P. Petersen, *Bioorg. Med. Chem. Lett.,* 1999, **9**, 1459; (f) W. E. Rose and M. J. Rybak, *Pharmacotherapy*, 2006, **26**, 1099.
18. P. P. Giovannini, G. Fantin, A. Massi, V. Venturi and P. Pedrini, *Org. Biomol. Chem.,* 2011, **9**, 8038 and references therein.
19. For approaches based on direct C-C bond formation, see: (*a*) C. A. Rose, S. Gundala, C.-L. Fagan, J. F. Franz, S. J. Connon and K. Zeitler, *Chem. Sci.,* 2012, **3**, 735; (*b*) O. Bortolini, G. Fantin, M. Fogagnolo, P. P. Giovannini, V. Venturi, S. Pacifico and A. Massi, *Tetrahedron*, 2011, **67**, 8110. For selected examples of more elaborated oxidative strategies, see: (*c*) J. Christoffers, *J. Org. Chem*., 1999, **64**, 7668; (*d*) A. M. R. Smith, H. S. Rzepa, A. J. P. White, D. Billen and K. K. Hii, *J. Org. Chem*., 2010, **75**, 3085 and references therein.
20. (*a*) P. P. Giovannini, P. Pedrini, V. Venturi, G. Fantin and A. Medici*, J. Mol. Catal. B: Enzym.*, 2010, **64**, 113; (*b*) O. Bortolini, P. P. Giovannini, S. Maietti, A. Massi, P. Pedrini, G. Sacchetti, V. Venturi, *J. Mol. Catal. B: Enzym.*, 2013, **85-86**, 93.
21. (*a*) P. Lehwald, M. Richter, Caroline Röhr, H.-w. Liu and M. Müller, *Angew. Chem., Int. Ed.,* 2010, **49**, 2389; (*b*) M. Müller, G. A Sprenger and M. Pohl, *Curr. Opin. Chem. Biol*., 2013, **17**, 261-270.
22. U. T. Bornscheuer, *Angew. Chem., Int. Ed.,* 2003, **42**, 3336.
23. H. H. Weetal, *Methods in Enzymology*, ed.: K. Mosbach, Academic Press, New York, 1976, **44**, pp. 134.
24. (*a*) A. L. Ahmad, E. M. Low and S. R. A. Shukor, *J. Mol. Catal. B: Enzym*., 2013, **88**, 26; (*b*) R. Lin, R. Wu, X. Huang and T. Xie, *Prep. Biochem. Biotechnol.*, 2011, **41**, 154; (*c*) L. Lloret, F. Hollmann, G. Eibes, G. Feijoo, M. T. Moreira and J. M. Lema, *Biodegradation*, 2012, **23**, 373.
25. M.-C. Yen, W.-H. Hsu and S.-C. Lin, *Process Biochem*., 2010, **45**, 667.
26. (*a*) M. Guillén, M.D. Benaiges and F. Valero, *Biotechnol. Progr.,* 2011, **27**, 1232; (*b*) M. J. Hernaiz, and D. H. G. Crout, *Enzyme Microb. Technol.,* 2000, **27**, 26.
27. W. J. Ting, K. Y. Tung, R. Giridhar and W. T. Wu, *J. Mol. Catal. B: Enzym.,* 2006, **42**, 32.
28. (*a*) A. M. Girelli, E. Mattei and A. Messina, *Sens. Actuators, B,* 2007, **121**, 515; (*b*) G. Felix, V. Descorps, *Chromatographia*, 1999, **49**, 595.

29. A slow but detectable decomposition of **1a** was observed in phosphate buffer (pH 6.5); the mechanism of this undesired side reaction is currently under investigation.
30. According to literature reports, we assumed that the absorbance at 280 and 215 nm of a 1% solution of the protein ($A_{280}^{1\%}$ and $A_{215}^{1\%}$) equals 13 and 200, respectively. The given values of protein concentration (Tables 1 and 2) result from the average of spectrophotometric measurements carried out at the above wavelengths. (*a*) W. J. Waddell, *J. Lab. Clin. Med*., 1956, **48**, 311; (*b*) C. N. Pace, F. Vajdos, L. Fee, G. Grimsley and T. Gray, *Prot. Sci.,*1995, **4**, 2411.
31. J. Christoffers, T. Kauf, T.Werner and M. Rössle, *Eur. J. Org. Chem.,* 2006, 2601.
32. C. Clausen, I. Weidner and H. Butenschön, *Eur. J. Org. Chem.,* 2000, 3799.
33. R.M. McCormick and B.L. Karger, *Anal. Chem.,* 1980, **52**, 2249.
34. F. Gritti, Y. Kazakevich and G. Guiochon, *J. Chromatogr. A,* 2007, **1161**, 157.